



Optimization of Hybrid Core Designs in 3D-Printed PLA+ Sandwich Structures: An Experimental, Statistical, and Computational Investigation Completed with Bibliometric Analysis

Zaineb Waired Metteb¹, Ahmed Ali Farhan Ogaili^{1*}, Kamal Abdulkareem Mohammed¹, Ahmed Mohsin Alsayah³, Mohsin Noori Hamzah², Zainab T. Al-Sharify⁴, Alaa Abdulhady Jaber³, Emad Kadum Njim⁵

¹Mustansiriyah University, Baghdad, Iraq

²University of Technology, Baghdad, Iraq

³The Islamic University, Najaf, Iraq

⁴Al Hikma University College, Baghdad, Iraq

⁵State Company for Rubber and Tires Industries, Najaf, Iraq

*Correspondence: E-mail: ahmed_ogaili@uomustansiriyah.edu.iq

ABSTRACT

This work presents the experimental test and Finite Element Analysis (FEA) of six core profiles (i.e. Square, Circle, Ellipse, Octagon, Pentagon, and Hexagon grids) on mechanical properties of 3D-printed Polylactic Acid Plus (PLA+) sandwich panels. Tensile and flexural tests were carried out to evaluate the structural performance of each core geometry; FEA in Abaqus was employed to study the stress distribution and deformation patterns. In contrast, the mechanical properties were the highest for the hexagonal and pentagonal cores with tensile strengths of 45.2 and 43.8 MPa, respectively, and flexural strengths of 290 and 323 MPa, respectively. ANOVA and Tukey's HSD tests indicated that core geometry significantly influences the flexural strength of sandwich panels of 0.94. The new hybrid hexagonal-octagonal core geometry was henceforth proposed to continue the quest for structural efficiency. The integration of the experimental and numerical approaches in such a way that validates the reliability of the FEA model itself gave less than 6% error in predicting flexural strength.

ARTICLE INFO

Article History:

Submitted/Received 20 Dec 2024

First Revised 19 Jan 2025

Accepted 23 Mar 2025

First Available Online 24 Mar 2025

Publication Date 01 Sep 2025

Keyword:

3D printing,

Core structures

FEA,

Flexural modulus,

PLA+,

Tukey's HSD.

1. INTRODUCTION

In recent years, sandwich composite structures have garnered significant attention in engineering due to their exceptional mechanical properties, including high strength-to-weight ratios, energy absorption, and load distribution capabilities [1–2]. They usually comprise two thin, highly-reinforced panels with a light core sandwiched between them. While the face panels are usually composed of composites, metals, or polymers, the core often comprises materials like foam, honeycomb, or balsa wood. Sandwich composites' structural efficiency has made them extremely valuable in sectors where weight reduction and structural efficiency are the most important considerations (i.e., the automotive, aerospace, and renewable energy systems sectors) [3,4]. Traditional core materials are, however, typically constrained by geometric design and manufacturing complexity constraints [5]. Additive manufacturing (AM) technology enables intricate, topology-optimized core geometries in sandwich panels that were previously impossible to manufacture [6,7]. FDM is a very accurate and simple AM process that is appropriate for complicated thermoplastics like PLA+ [8]. PLA+ stands out for being an advanced form of standard PLA with increased mechanical properties that make it suitable for structural applications. Recent research demonstrated that 3D-printed PLA+ parts can be comparable to traditional materials when optimized by parameter tuning such as layer height, infill density, and raster angle [9–11]. A crucial knowledge gap, however, lies in the understanding of the effect of core geometry non-traditional polygonal (pentagonal, octagonal) and curvilinear (elliptical, circular) on the mechanical performance of PLA+ sandwich panels. Hexagonal and honeycomb cores are commonly reported for energy absorption and compressive strength. Still, new studies suggest that hybrid and irregular geometries can facilitate better performance by minimizing stress concentrations and optimizing load redistribution [12]. For instance, triply periodic minimal surface (TPMS) cores, such as gyroid structures, have exhibited superb energy absorption under dynamic loading, while novel lattice geometries have shown promise in balancing manufacturability with structural efficiency [13]. Despite these advances, comparative research on different core profiles remains scarce, particularly those integrating experimental validation with computational simulation to include material anisotropy and geometric nonlinearity [14]. The mechanical behavior of sandwich panels is highly dependent on core architecture, which governs load transfer, energy dissipation, and overall structural efficiency. Previous studies have highlighted the role of core geometry in optimizing mechanical properties such as compressive strength, bending stiffness, and energy absorption [15,16]. Honeycomb and hexagonal cores provide superior energy absorption and compressive strength thanks to their geometric stability. Traditional core geometries can compromise manufacturability for structural optimization and therefore might not fulfill their full potential for high-performance applications [17]. Hybrid core geometries, integrating the benefits of several lattice geometries, have exhibited potential in the improvement of structural efficiency. For instance, a hybrid steel-polymeric lattice core exhibited an optimized strength-to-weight ratio and customizable mechanical response. Aluminum honeycomb infill in square tubes also enhanced energy absorption under dynamic loading. Even with these developments, systematic analyses of hybrid core designs in 3D-printed PLA sandwich panels are scant [18]. FEA has emerged as a key tool in predicting mechanical behavior in sandwich panels, especially under complex loading conditions. However, differences between simulation predictions and experimental observations frequently occur on account of material nonlinearity, complexities in boundary conditions, and imperfections in geometry. Recent research has tried to address these issues with advanced techniques of modeling, such as the

use of the Iwan model for simulating the viscoelasticity of core materials. For example, Validated FEA simulations for 3D-printed PLA composites in one study were found to yield reasonable accuracy for tensile strength but with increased errors for flexural analysis. Also, it was shown through another study that the core topology plays a major role in the mechanical behavior of 3D-printed sandwich panels with some lattice patterns yielding significantly higher strength and stiffness than the conventional honeycomb patterns [19]. Despite these developments, the combination of numerical modeling and experimental verification remains a formidable challenge for the design of sandwich panels. Statistical testing, including analysis of variance (ANOVA) and post-hoc testing (e.g., Tukey's HSD), must be used to describe the effect of core geometry upon the mechanical properties of sandwich composites. These allow systematic means for the optimization and verification of performance gains. ANOVA, for instance, was used to determine the effect of core topology upon flexural strength, where effect sizes (η^2) described the strength of these correlations [20]. When analyzing the study of natural fiber-reinforced epoxy composites, ANOVA identified the orientation and type of fibers significantly affected tensile and impact strength, illustrating the requirement for the use of statistical verification within the design of composites [21]. Hybrid core geometries involving two or more geometric features or materials have emerged as a desirable approach for the improvement of structural efficiency. A recent article described a novel ultralight multifunctional sandwich structure with an N-H hybrid core combining micro-perforated face sheets with a hybrid core for enhanced sound absorption and load-carrying ability. The hybrid design took advantage of synergistic interaction between material properties and core geometries and exhibited superior dynamic and static loading performance [22]. In the same way, hybrid lattice cores with periodic and aperiodic geometries have shown potential for stiffness and energy dissipation optimization for aerospace. The developments validate the merit of bringing statistical rigor and novel core geometries into the solution of demanding engineering issues [23]. Through the exploration of the interaction between core topology, material properties, and mechanical behavior through systematic study, scientists can design optimized sandwich structures for use in anything from renewable energy systems to lightweight vehicle components. A single design, have shown potential for enhanced structural performance. For instance, a novel hexagonal-octagonal core geometry presented here aims to capture the superior mechanical properties of hexagonal patterns while improving manufacturability and structural efficiency.

The originality of the present work consists in the fact that it provides a full comprehension of the structural behavior of PLA+ sandwich panels by employing experimental and numerical techniques, gaining insights into their optimal design and further usage within various industrial sectors. This study adds to the field in the following manner:

- (i) Mechanical Benchmarking: A methodical comparison of six fundamental geometries (square, circular, elliptical, octagonal, pentagonal, and hexagonal grids) to determine optimum configurations for high-stress applications, filling a significant gap in the literature that is filled with traditional honeycomb and grid structures.
- (ii) Hybrid Core Innovation: The creation of a hexagonal-octagonal hybrid core, which seeks to balance structural efficiency with geometric complexity, provides an innovative solution for sustainable engineering.
- (iii) Methodological Integration: A rigorous validation framework spanning experimental testing, FEA, and sophisticated statistical analysis that furnishes a reproducible roadmap for future research in additive-manufactured composites.

By revealing the contribution of core topology to mechanical performance, this work propels the development of high-strength, lightweight sandwich panels, meeting global sustainability objectives via less material waste and energy use.

This paper is important, as shown by excellent trends in publication (see **Figure 1**). Detailed information on how to get bibliometric analysis data using Scopus is explained elsewhere [24-26]. **Figure 1** shows the number of research articles per annum between 2017 and 2025 on 3D-printed PLA+ sandwich structures, based on Scopus data. The research grew consistently, hitting the peak number of 20 articles in 2023, perhaps due to advances in 3D printing and the demand for lightweight materials. The dip in 2024 and 2025 is slight and suggests a possible shift in focus or saturation of the market. This trend suggests the ongoing importance of optimizing core geometries to attain better structure performance in the aerospace and car sectors.

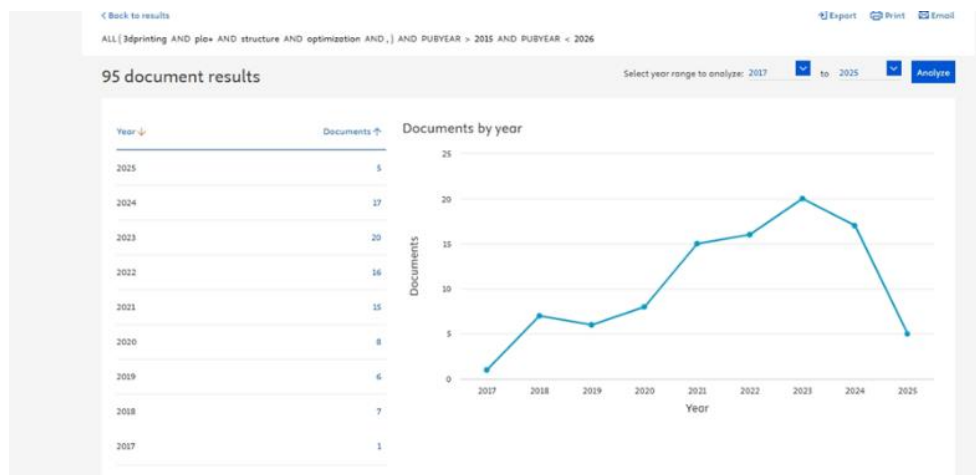


Figure 1. Research trend using keywords “3d-printed, PLA+, Sandwich and Structure” taken on 2025.

2. METHODS

2.1. Material Selection

PLA+ was used in this study due to its enhanced mechanical properties, biodegradability, and suitability for 3D printing applications. PLA+ is a high-performance version of the standard Polylactic Acid (PLA) featuring a higher tensile strength, rigidity, and resistance to impact. PLA+ is derived from renewable resources such as corn starch or sugarcane and is hence an environmentally friendly thermoplastic, meeting the growing demand for sustainable manufacturing solutions [27]. Material properties of PLA+ make it especially fit for structural applications, including the making of sandwich panels. The PLA+ in this study has very high tensile strength compared to a standard PLA sample. These properties outperform the corresponding properties of regular PLA, whose tensile strength generally is, and Young's modulus of [28]. Besides, PLA+ can be combined with Fused Deposition Modeling (FDM) 3D printing, which gives the possibility for complex geometries in high precision with minimal material waste.

In the present study, 1.75 mm diameter filaments of consistent quality were used and obtained from a well-established manufacturer. Concerning the thermal properties, the material has to be considered for the optimization of parameters for 3D printing: its glass transition temperature of 60–65°C and the melting temperature of 150–160°C. The selection of PLA+ as the main material was further justified because it is easy to process, has a low warping tendency and produces parts with smooth surface finishes.

2.2. Core Profile Design Methodology

The core profile design is treated as one of the major parts of this research since the geometrical arrangement of the core structure plays a crucial role in the mechanical behavior of the sandwich panel in total. This study investigates six core profiles with different geometrical features, hence giving some potential structural benefits. Several shapes under study are Square, Circles, Ellipse, Octagon, Pentagon, and Hexagon patterns, as shown in **Figure 2**. The most basic configuration concerns the Lines, where parallel and vertically oriented supports are set indeed a benchmark for each geometry that goes a little fancier. This pattern results in direct methods of verticals that provide very supportive resistive performances, especially because the nature of the line structure is subjected to compression within a more massive rigid body. Consequently, work on the pattern of Circles introduces structural features with curved materials that can distribute in situ stress favorably between more uniform dispersions throughout that structure. Second to the circled pattern is an extension of applying such curved geometric features to ellipse-like shapes, giving way to elongations that indeed would increase this bending resistance oriented toward particular symmetrical axes across space.

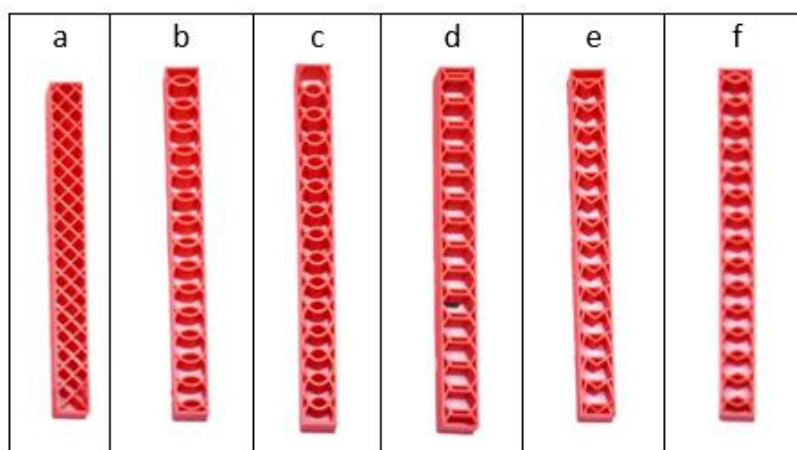


Figure 2. Sample different core profile.

The polygonal patterns for the Octagon, Pentagon, and Hexagon investigate various angular geometries and the resultant effect such geometry has on structure performance. Because the shape is eight-sided in the Octagon pattern, one could expect enhanced performance due to the greater range of load pathways, hence the superior capacity for resisting multi-directional forces. From another perspective, an interesting balance between angular and more rounded load transmission creates a fascinating Pentagon pattern, while from nature, efficiency in material consumption and flow of load under a hexagonal pattern is advantageous. All the components were designed using SOLIDWORKS 2023 computer-aided design software to ensure that all the test specimens had precisely controlled dimensions and geometric accuracy.

Table 1 presents the standardized dimensions of the PLA+ sandwich panel components that were used in this study. These are the length (150 mm), width (50 mm), thickness of the top skin (2 mm), thickness of the core (6 mm), thickness of the bottom skin (2 mm), and total thickness (10 mm). These were selected with careful consideration to be uniform in all the test specimens. Hence, there is a fair comparison of the mechanical properties with various core geometries. The length was selected as 150 mm to be in the direction of loading, and the width was selected as 50 mm to ensure uniform stress during testing. The sandwich panel

samples from top and bottom skin thicknesses were suggested as 2 mm for the required rigidity. In comparison, the core thickness was selected as 6 mm to ensure a compromise between structural integrity and weight. The 10-mm thickness ensures that the sandwich panels are rigid enough. Hence, they can be endured during mechanical testing without excessive deformation. These standard dimensions play a crucial role in ensuring that the experimental results are reproducible and can be compared with various core geometries. The uniformity in the dimensions also ensures that the (FEA) simulations can be properly done, as the models can be directly compared with the actual test specimens. This table is a reference point for the experimental setup and ensures that all the test specimens are prepared in the same conditions, reducing the variability in the results.

Table 1. Standardized dimensions of PLA+ sandwich panel components.

Parameter	Dimension (mm)	Description
Length	150	Parallel to the loading direction
Width	50	Perpendicular to the loading direction
Upper Skin Thickness	2	Outer surface layer
Core Thickness	6	Internal structural component
Lower Skin Thickness	2	Base surface layer
Total Thickness	10	Complete sandwich assembly

The design process involved several key steps to ensure manufacturability and consistency:

- (i) Geometrical modeling in SOLIDWORKS should be done with much care at the beginning to hold the wall thickness uniform without any sharp corners that may cause a stress concentration.
- (ii) Export the designs as STL (Standard Tessellation Language) files, preserving the geometric accuracy of the models.
- (iii) Processing with Ulti maker Cura slicing software to produce manufacturable G-code.
- (iv) Implementation of consistent printing parameters, such as a 20% infill density across all core profiles, ensures valid comparisons.

In all designs, the wall thicknesses and void ratios were kept constant to maintain the integrity of observed performance due to changes in geometric configuration rather than by material distribution. The 20% infill density was chosen as an optimum value for balancing material usage with structural integrity, providing enough support and maintaining typical characteristics for each core profile. This parameter has been kept constant for all designs to insulate the effect of geometric patterns on mechanical performance. These designs represent a systematic study of the core geometry-sandwich panel performance relationship, and indeed, each pattern shows promise for performance advantages under different loading conditions or in particular applications. Further sections discuss in detail how these geometrical variations influence mechanical performance differences when flexural loading conditions are applied.

2.3. Core Profile Design Challenges

All the core profiles were designed with proper consideration of both manufacturing constraints and principles of design. This section describes the methodological procedure for each profile arrangement with specific problems faced during the manufacturing and designing process. **Figure 2** shows the cross-sectional profiles for the six core profiles that were studied in this work: square, circular, ellipsoidal, octagon, pentagon, and Hexagonal grids. Each core profile is designed with special geometric properties to investigate the impact on the mechanical performance of the PLA+ sandwich panels.

- (i) Square Grid: A square grid consists of parallel vertical supports in the shape of a grid pattern. This structure provides an easy way for the distribution of the load but is subject to stress concentrations at the grid line intersections.
- (ii) Circles Grid: Circles grid comprises concentric circular elements with more even sharing of stress than linear structures. However, stress concentrations can be identified at the circle intersections.
- (iii) Ellipse Grid: The ellipse grid is an extension of the circle's grid, with elongated elliptical elements providing directionality to the optimization of the strength. This structure is particularly effective at resisting bending along specific axes.
- (iv) Octagon Grid: The Octagon grid uses an eight-sided geometric pattern to provide resistance in many different orientations. The complexity of this structure requires precise manufacturing to provide structural stability.
- (v) Pentagon Grid: Pentagon elements with five sides are employed in the Pentagon grid to achieve angular and rounded loading transmission. It is efficient in reducing stress concentrations at the vertex.
- (vi) Hexagonal Grid: A hexagonal grid utilizes elements with six sides to achieve the most efficient loading distribution. It is renowned for its even loading distribution and is widely used in structural engineering.

All base profiles were developed using SOLIDWORKS 2023 and produced using FDM 3D printing techniques. The proposed geometric complexity of each profile was taken into careful account to attain manufacturability and structural function. It distinguishes the unique geometric patterns and their spatial arrangement, developing a visual representation of the core profiles used in this study.

2.4. Specimen Fabrication

The sandwich panels were printed using a Creality Ender 3D printer, which allowed for precise layering and material control. Not only did this allow for reduced waste, but it also enabled the creation of complex geometries that traditional manufacturing methods were unable to produce. 3 Pro 3D printer, which is an FDM technology printer. FDM is the most common additive manufacturing method and uses the extrusion of thermoplastic filaments through a hot nozzle. It layers the material and constructs a three-dimensional object.

Table 2 shows the printing parameters utilized in the printing of the PLA+ sandwich panels in this study. The parameters are nozzle temperature (210°C), bed temperature (60°C), layer height (0.2 mm), print speed (60 mm/s), infill density (20%), filament diameter (1.75 mm), and status of the cooling fan (on). The parameters were chosen with caution to achieve high-quality prints with the lowest amount of defects, such as delamination and warping. A 210°C nozzle temperature was chosen to achieve the optimal viscosity for the extrusion of the PLA+, while a 60°C bed temperature was used to achieve good adhesion of the first layer on the build platform. A layer height of 0.2 mm provides the balance between the resolution of the prints and the printing time, while a printing speed of 60 mm/s provides the uniform deposition of the material. An infill density of 20% was used to balance the consumption of the material and the structural integrity, providing the necessary support to the sandwich panels with the use of the lowest level of the material. A filament diameter of 1.75 mm is typical for FDM printing, and the cooling fan was enabled to hasten the solidification process and reduce warping.

All the parameters were fixed for all the core profiles to have the same manufacturing conditions and a valid comparison of the mechanical performance.

Table 2. Printing parameters for PLA+ sandwich panels.

Parameter	Value
Nozzle Temperature	210°C
Bed Temperature	60°C
Layer Height	0.2 mm
Print Speed	60 mm/s
Infill Density	20%
Filament Diameter	1.75 mm
Cooling Fan	Enabled

Printing was performed in a single stage where the core and outer skins were printed together. This method has provided good adhesion among layers with minor defects like delamination and warping. The specimens were then inspected for dimensional accuracy and surface quality after printing. Defective samples were removed to maintain the integrity of experimental results.

2.5. 3D Printing Techniques

The main 3D printing technique that was used in the present work was Fused Deposition Modeling. FDM is a quite affordable and widely available method of additive manufacturing, which is ideal for prototyping and small production. It includes the process of feeding the thermoplastic filament through the heated nozzle and melting the fed material by depositing it layer by layer on the build platform. These then solidify into a 3D object upon cooling. Mainly, the advantages of the FDM process are that complex geometries can be fabricated, material waste is minimized, and parts with good mechanical properties are obtained. However, for producing high-quality prints, such problems as layer adhesion, warping, and surface roughness have to be overcome. In this process, such problems were reduced by optimizing printing parameters like nozzle temperature, bed temperature, and print speed [29]. **Figure 3** provides a schematic representation of the FDM process used to fabricate the PLA+ sandwich panels in this study. The FDM process involves the extrusion of thermoplastic filaments through a heated nozzle, which deposits the material layer by layer to form a three-dimensional object.

- (i) Filament Feeding: The PLA+ filament is fed into the FDM printer, where it is heated to a temperature of 210°C to achieve the desired viscosity for extrusion.
- (ii) Nozzle Extrusion: The heated filament is extruded through a nozzle with a diameter of 0.4 mm, depositing the material onto the build platform in a controlled manner.
- (iii) Layer-by-Layer Deposition: The material is deposited layer by layer, with each layer having a thickness of 0.2 mm. The print speed is set to 60 mm/s to ensure high-quality prints with minimal defects.
- (iv) Cooling and Solidification: After deposition, the material cools and solidifies, forming a solid structure. The cooling fan is enabled to accelerate the solidification process and reduce warping.

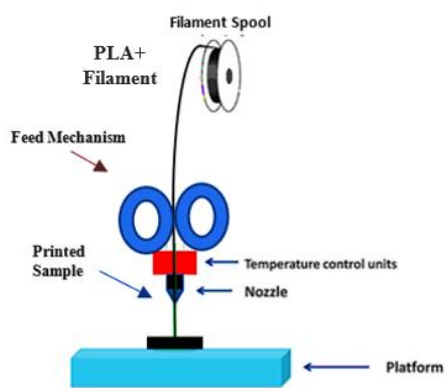


Figure 3. Fused Deposition Modeling (FDM) process.

2.6. Experimental Testing

The objective of this experimental research was to evaluate the structural behavior of PLA+ sandwich panels by mechanically testing them under various core configurations. To obtain accurate and repeatable results, all the testing was conducted in a controlled laboratory setting of $25 \pm 2^\circ\text{C}$ and $50 \pm 5\%$ relative humidity, following the applicable ASTM standards. The goal of the test program was to evaluate the tensile and flexural behavior of the sandwich panels, which would give valuable insight into the response of the mechanical components under various stress conditions.

2.6.1. Tensile testing methodology

The mechanical performance of PLA+ samples with different core geometries was evaluated by uniaxial tensile testing as shown in **Figure 4**. The experimental procedure was based on the ASTM D638-14 standard [30], with some modifications to adapt to the particular structural features of sandwich composites, according to recent work like [31-32]. The tests were designed to determine the main mechanical properties such as tensile strength, elastic modulus, and elongation at break, and to provide information on the failure mechanisms and strain distribution patterns at the speed of the load 2 mm/min as recommended in previous work procedures [33,34].



Figure 4. Tensile test of PLA+ samples.

2.6.2. Flexural testing methodology

The flexural performance of PLA+ sandwich panels with different geometries of the core segment was studied in a flexural test as shown in **Figure 5**. From the Figure, tests were conducted following standard ASTM D790-17 [35], with supplementary adjustment to reflect specific structural features of sandwich composite materials according to recent studies [36–

38]. The experimental setup and testing protocol have been designed and devised to measure the key flexural properties, such as flexural strength, flexural modulus, and failure modes, providing insight into the deformation behavior of the sandwich panels. Flexural tests were performed using an Instron 5982 universal testing machine equipped with a 10 kN load cell and advanced displacement control capabilities. The three-point bending setup included:

- (i) Support span (L): 120 mm (16:1 span-to-thickness ratio).
- (ii) Loading rate: 2 mm/min (selected to ensure quasi-static loading conditions).
- (iii) Maximum deflection: L/2 (12 mm).
- (iv) Roller diameter: 10 mm (to minimize stress concentrations at contact points).

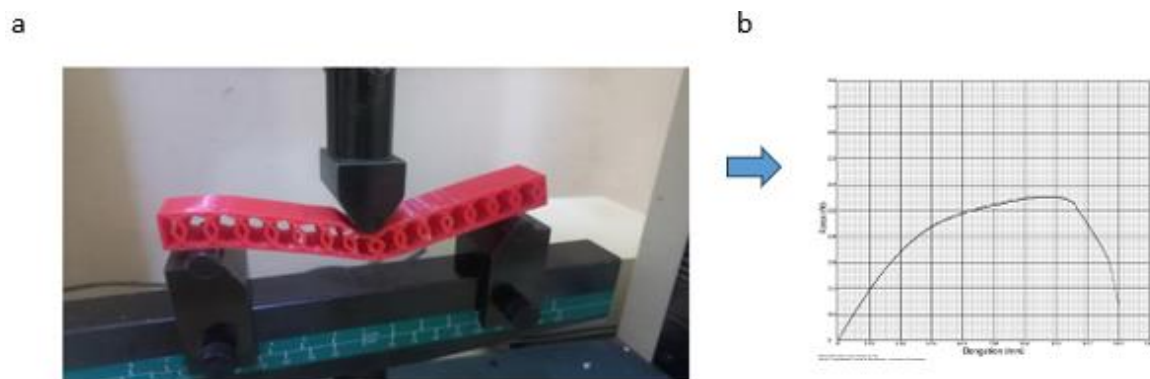


Figure 5. a) Flexural test setup, b) load - deformation result.

Mechanical properties of the PLA+ sandwich panels under flexural loading were derived from the load-deflection data obtained during the three-point bending tests. The following parameters were calculated to evaluate the flexural performance of the specimens:

- (i) Flexural strength (σ_f): The flexural strength represents the maximum stress the material can withstand before failure under bending conditions [39]. It is calculated using the modified beam theory equation (1):

$$\sigma_f = \frac{3PL}{2bd^2} \quad (1)$$

where P is the applied load (N), L is the support span (mm), b is the specimen width (mm), and d is the specimen thickness (mm).

- (ii) Flexural modulus (E_f): The flexural modulus is a measure of the material's stiffness under bending conditions. It is calculated from the initial slope of the load-deflection curve using the following equation (2):

$$E_f = \frac{mL^3}{4bd^3} \quad (2)$$

where: m = Slope of the load-deflection curve (N/mm), L = Support span (mm), b = Specimen width (mm), d = Specimen thickness (mm).

The flexural modulus quantifies can be defined as the ability of material to resistance deformation under bending loads and it is one of a keys parameter for structural design applications. Higher values of E_f indicate greater stiffness and rigidity.

2.7. Finite Element Analysis (FEA) Methodology

FEA was performed using ABAQUS/CAE 2017 to simulate the mechanical behavior of PLA+ sandwich panels under flexural loading. The FEA methodology was designed to complement the experimentally obtained results by affording greater insight into stress distribution patterns, deformation mechanisms, and the prevailing modes of failure [40,41]. Numerical simulations considered geometric and material nonlinearities to accurately predict a structure's response.

2.7.1. Model development

FEA models were developed to simulate the mechanical response of PLA+ sandwich panels under flexural loading. The models incorporate geometric and material nonlinearities for accurately predicting structural responses. This involves material parameters, finite element mesh, and boundary conditions to mimic the experimental setup in **Figure 6**. FEA models made from the six core profiles studied in this work are presented in **Figure 6**: Square grid, Circles grid, Ellipse grid, Octagon grid, Pentagon grid, and Hexagon grid. Subfigure (a) to (f) is the FEA model for each core profile, representing the material and geometric nonlinearities used in the simulations. Models were established with ABAQUS/CAE 2017 to simulate the mechanical response of the PLA+ sandwich panels subjected to flexural loading. FEA models make use of the unique geometric feature in each core profile, including the parallel vertical supports in the square grid (a), the concentric circle elements in the Circles grid (b), the elongated elliptic elements in the Ellipse grid (c), the multi-directional support in the Octagon grid (d), the five-sided elements in the Pentagon grid (e), and the six-sided honeycomb pattern in the Hexagon grid (f). Models are finely meshed to capture the stress concentrations and the pattern of deformations, with special care in the critical locations such as intersections and vertices. The boundary conditions reproduce the experimental three-point bending setup, with the ends constrained and with the middle load applied to mimic flexural loading.

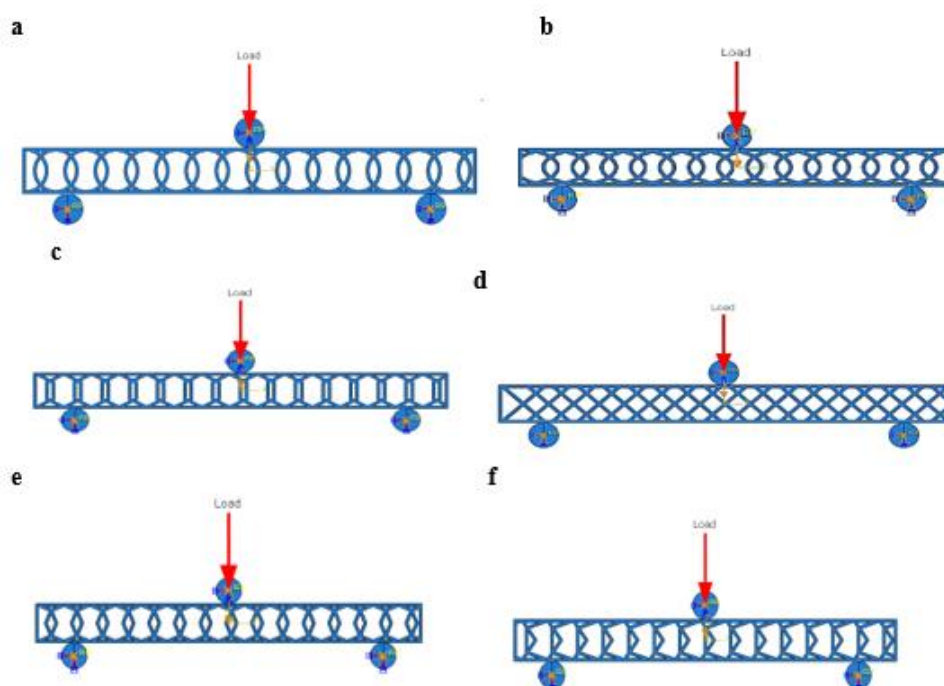


Figure 6. Flexural beam simulated for the several samples.

2.7.2. Mesh characteristics

One of the most critical components of the FEA process is the finite element mesh, which has a direct influence on the accuracy and reliability of the results [42]. In the design of the mesh, a good balance between computational efficiency and the capability to capture the distribution of complex stresses, modes of deformation, and failure modes must be achieved [43]. In this study, the mesh was carefully tailored to the geometric complexity of each core profile in a way that balanced accuracy and computational feasibility as shown in **Figure 7**. The finite element mesh applied to the six core profiles is shown in **Figure 7**: Square grid (a),

Circles grid (b), Ellipse grid (c), Octagon grid (d), Pentagon grid (e), and Hexagon grid (f). The subfigures show the mesh distribution in accordance with the geometric complexity of the respective core profile. The mesh is enriched in critical zones, such as vertices and intersections, to accurately capture stress concentrations and deformation patterns. The use of C3D8R (8-node linear hexahedral) and C3D6 (6-node wedge) elements is a balance between computational cost and accuracy. Mesh convergence studies verified that the results were independent of the element size, with less than a 2% difference in stress and displacement values with further refinement. The above figure illustrates the need for a well-designed mesh in determining the mechanical response of PLA+ sandwich panels under flexural loading, ensuring that valid FEA results are obtained for all core profiles.

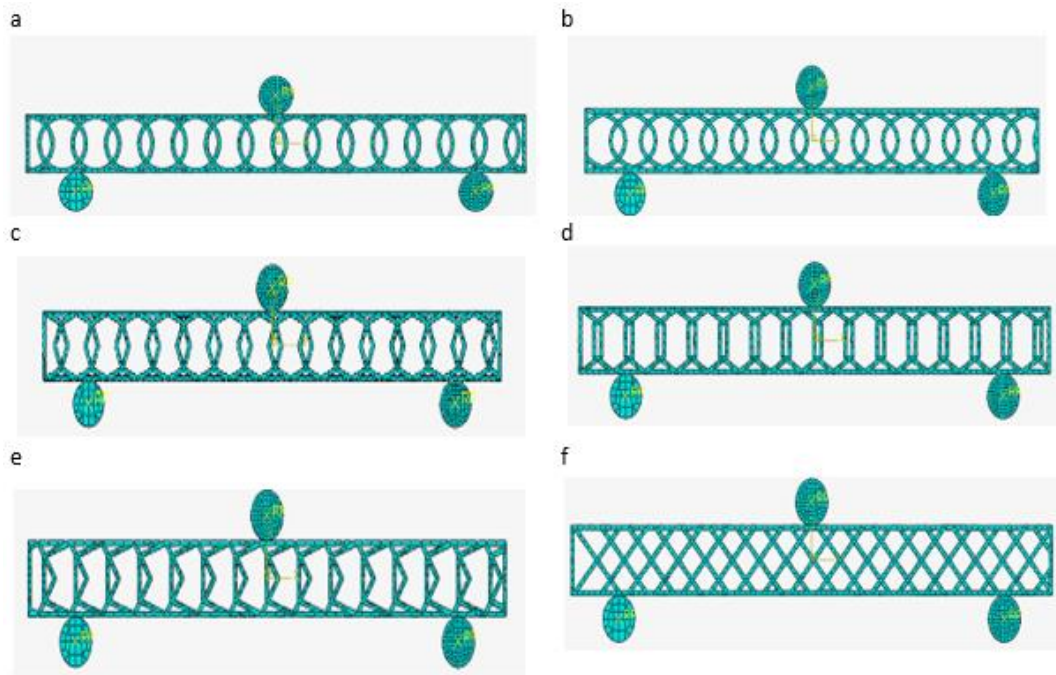


Figure 7. Mesh coverage for the model.

The following principles guided the mesh development:

- (i) **Element Type and Quality:** C3D8R (8-node linear hexahedral elements with reduced integration): These elements formed most of the model due to their computational efficiency and capability in capturing stress gradients. Reduced integration elements, in general, are very effective in large-scale simulations since computation costs are reduced without significant loss of reasonable accuracy. C3D6-6-Node linear wedge elements: This Wedge type can be applied since the geometric characteristics in many critical regions may contain geometries for hexahedral elements. The application using wedge elements proved to be feasible for all characteristic curvatures and detailed geometrical accuracies within every core profile; accurate conformity was implemented to avoid noticeable loss of the precise solution due to specific numerical approximation rather than losing computational time.
- (ii) **Mesh Convergence:** Convergence studies on mesh size were performed in order to ensure the independence of results from element size. The convergence criterion was less than a 2% change in maximum stress and displacement values for further refinement. This process, in detail, included progressive refining of the mesh in critical regions, like near loading points and interfaces, until the stabilization of results was

obtained, ensuring the fineness of the mesh was sufficient to correctly capture the stress and strain distributions.

- (iii) Aspect Ratio and Skewness Aspect ratio: The aspect ratio of the elements was kept below 3:1 in order to avoid numerical inaccuracies. Elements with high aspect ratios can lead to ill-conditioned stiffness matrices and result in poor predictions of stress and displacement.
- (iv) Skewness: The skewness of the elements was maintained at less than 0.3 in order to ensure high-quality meshing [44]. The skew elements can introduce errors in stress calculation, especially in the regions with a high stress gradient, so maintaining low skewness was required for the calculation of accurate results

2.7.3. Mesh Details for Each Core Profile

The mesh characteristics varied across the six core profiles due to differences in geometric complexity. **Table 3** summarizes the finite element mesh characteristics for the six core profiles, detailing the total nodes, elements, and distribution of C3D8R (8-node linear hexahedral) and C3D6 (6-node wedge) elements. Mesh design is critical for balancing computational accuracy and efficiency in finite element analysis (FEA). For the Circle grid, 9,648 nodes and 5,753 elements (4,565 C3D8R, 1,188 C3D6) prioritize curved geometry resolution. The Pentagon grid employs 4,696 nodes and 3,689 elements (1,722 C3D8R, 1,967 C3D6), emphasizing vertex stress mitigation. The Ellipse grid uses 5,616 nodes and 3,200 elements (2,896 C3D8R, 304 C3D6), optimizing directional strength with refined elongated regions. The Octagon grid features 9,438 nodes and 5,960 elements (4,050 C3D8R, 1,910 C3D6) to accommodate multi-directional loading. The Hexagon grid integrates 7,909 nodes and 4,980 elements (3,440 C3D8R, 1,540 C3D6) for uniform load distribution. The Square grid, with 11,220 nodes and 6,545 elements (5,764 C3D8R, 781 C3D6), focuses on grid intersection stress concentrations. C3D8R elements ensure computational efficiency in bulk regions, while C3D6 elements address geometric complexity in curved or angular zones. Mesh convergence studies confirmed minimal sensitivity to element size ($\leq 2\%$ variation), ensuring reliable predictions of stress and displacement. This structured approach underscores the necessity of tailored meshing strategies to accurately simulate mechanical behavior in 3D-printed PLA+ sandwich panels, providing a foundation for optimizing core geometries in structural applications.

Table 3. Mesh details for each core profile.

Core Profile	Total Nodes	Total Elements	C3D8R Elements	C3D6 Elements
Circle grid	9648	5753	4565	1188
Pentagon grid	4696	3689	1722	1967
Ellipse grid	5616	3200	2896	304
Octagon grid	9438	5960	4050	1910
Hexagon grid	7909	4980	3440	1540
Square grid	11220	6545	5764	781

2.7.4. Importance of Mesh Design

The mesh design is a cornerstone of FEA, as it directly impacts the accuracy of stress, strain, and displacement predictions. The following points highlight the importance of a well-designed mesh in this study:

- (i) Stress Gradient Capture. In regions with high stress gradients, such as near loading points and core-face sheet interfaces, a finer mesh is essential to accurately capture the stress

distribution. The stress (σ) at any point is calculated using the material stiffness matrix (D) and the strain tensor (ϵ) can be calculated from equation (3):

$$\sigma = D \cdot \epsilon \quad (3)$$

A coarse mesh in these regions can lead to underestimation of peak stresses, resulting in inaccurate failure predictions.

- (ii) Deformation Accuracy: One of the importance of the output result of simulation is the displacement field (u), which can be calculated from the principle of finite element approximation using equation (4):

$$u = \sum_{i=1}^n N_i u_i \quad (4)$$

where N_i is the shape functions, and u_i is the nodal displacements. Accurate representation of the displacement field is guaranteed by a sufficiently resolved mesh, especially in areas of complicated deformation patterns like the curved regions of the ellipse and circle profiles.

- (iii) Failure Prediction. For accurate prediction of failure modes like delamination and core crushing, a highly resolved mesh is needed in the zones of criticality. The von Mises stress criterion was employed to predict failure in the PLA+ material. The criterion, which is given by equation (5), calculates the equivalent state of stress and provides a good indication of material yielding for complicated states of loading.

$$\sigma_{vm} = \sqrt{\frac{(\sigma_1 - \sigma_2)^2 + (\sigma_2 - \sigma_3)^2 + (\sigma_3 - \sigma_1)^2}{2}} \quad (5)$$

where $\sigma_1, \sigma_2, \sigma_3$ are the principal stresses. A fine mesh in the interface regions ensured that localized stress concentrations were accurately captured, allowing for reliable failure predictions.

- (iv) Computational Efficiency. The use of reduced integration elements (C3D8R) and a balanced mesh density ensured that the simulations were computationally efficient without compromising accuracy. Reduced integration elements reduce the number of integration points, thereby decreasing the computational cost while maintaining reasonable accuracy. This is particularly important in large-scale simulations, where computational resources are a limiting factor.
- (v) Geometric Complexity. The geometric complexity of the core profiles, especially the hexagon and octagon patterns, required careful meshing to ensure that the stress distribution and deformation patterns were captured accurately. The use of wedge elements (C3D6) in these regions allowed for a high-quality mesh that conformed to the complex geometry without introducing numerical errors.

2.7.5. Challenges in mesh design

The following difficulties were encountered in the mesh design process, especially for the more complex core profiles:

- (i) Geometric Fidelity: The geometrical fidelity at the ellipse and pentagon profiles required very critical tuning of the mesh parameters, especially around the sharp corners and curved surfaces. The use of wedge elements, along with finer meshing in the critical areas, helped capture the geometry of the models correctly.
- (ii) Interlayer Bonding: The interface regions between the core and face sheets required a fine mesh in order to capture the stress concentrations and potential delamination. This was particularly challenging in the line and circle profiles, where the stress distribution was highly localized.

(iii) Computational resources: Another point was the mesh refinement-computational resources balance, due to the profile shapes that exhibited a very demanding number of elements, such as the hexagon and octagon to receive acceptable results concerning stress distribution. An application of reduced integration elements and balanced density mesh managed this problem.

However, from this, what can be drawn is that mesh design is one of the most important ingredients in analyses that need to be performed with due consideration to ensure that accuracy and reliability for FEA results are ensured by cautious tailoring of mesh to each geometrically complex core profile. Optimization is done further of the element type, density, and quality. The research thus correctly forecasts the distribution of stresses, deformation patterns, and modes of failure in the PLA+ sandwich panels. Knowledge gathered during the design of the mesh is therefore useful in future works dealing with optimization issues of 3D-printed sandwich structures.

2.7.6. Validation of FEA Model

Validation of the FEA model is the most essential step towards the reliability and accuracy of the numerical simulations. FEA results are validated here by comparing the simulated stress distribution, patterns of deformation, and modes of failure with the experimental results obtained from tensile and flexural tests. The major metrics of interest employed during the validation were load-deflection curves, patterns of stress distribution, and modes of failure. The agreement between the experimental results and the simulations ensured the validity of the FEA model.

2.8. Statistical Analysis Methodology

The investigation of core geometry's influence on the mechanical properties of Polylactic Acid Plus (PLA+) sandwich panels employed a rigorous statistical methodology designed to provide comprehensive insights into group-level variations and inter-group differences.

2.8.1. One-Way Analysis of Variance (ANOVA)

The primary analytical technique utilized was One-Way Analysis of Variance (ANOVA), a powerful statistical method for decomposing total variability into between-group and within-group components [45]. The ANOVA model can be mathematically represented in equation (6):

$$Y_{ij} = \mu + \alpha_i + \epsilon_{ij} \quad (6)$$

where Y_{ij} represents the observed flexural strength, μ is the grand population mean, α_i represents the effect of the i -th core geometric profile, and ϵ_{ij} denotes the random error term.

The ANOVA test statistic (F) was calculated using the following equation (7):

$$F = \frac{MS_{\text{mawn}}}{MS_{\text{nuthen}}} = \frac{\sum_{i=1}^k n_i (\bar{X}_i - \bar{X})^2 / (k-1)}{\sum_{k=1}^k \sum_{j=1}^m (X_{yj} - X_i)^2 / (N-k)} \quad (7)$$

where k is the number of groups (core geometric profiles), n_i is the sample size of the i -th group, \bar{X}_i is the mean of the i -th group, \bar{X} is the overall mean, and N is the total sample size.

2.8.2. Tukey's Honestly Significant Difference (HSD) post-hoc test

To systematically identify specific pairwise differences between core profiles, Tukey's Honestly Significant Difference (HSD) test was implemented [46]. The Tukey HSD statistic is computed in equation (8):

$$q = \frac{\bar{x}_i - \bar{x}_j}{SE} \tag{8}$$

where \bar{X}_i and \bar{X}_j are the means of two groups being compared, and SE is the standard error of the difference between group means.

2.8.3. Statistical assumptions and validation

The analysis was predicated on three fundamental assumptions critical to the validity of parametric testing [47]:

- (i) Normality of Distribution: The Shapiro-Wilk test was employed to validate the normality of residuals. The test statistic W is defined as shown in equation (9):

$$W = \frac{(\sum_{i=1}^n a_i(x_{(i)}))^2}{\sum_{i=1}^{n-1} (x_i - \bar{x})^2} \tag{9}$$

- (ii) Statistical significance was established at $p > 0.05$, ensuring conformity with the normal distribution assumption.
- (iii) Homogeneity of Variances: Levene's test assessed the equivalence of variance across experimental groups [48]. The test statistic W is calculated by using equation (10)

$$W = \frac{(N-k)\sum_{j=1}^k n_j(Z_j - Z_j)^2}{(k-1)\sum_{j=1}^k \sum_{i=1}^{n_j} (Z_j - Z_i)^2} \tag{10}$$

where Z_{ij} represents the absolute deviation from group means.

- (iv) Independence of Observations: Experimental design rigorously ensured the independence of each specimen through standardized manufacturing and testing protocols.

3. RESULTS AND DISCUSSION

3.1. Tensile Test Results

Tensile tests were conducted on PLA+ sandwich panels with six distinct core profiles to evaluate their mechanical performance under uniaxial loading. The tensile strength and Young's modulus for each profile are summarized in **Table 4** and visualized in **Figure 8**. The results highlight significant variations in mechanical behavior attributable to differences in core geometry, emphasizing the critical role of structural design in optimizing load-bearing capacity.

Table 4 observes that the hexagon core demonstrated the highest tensile strength (45.2 MPa) and stiffness (3.8 GPa), thanks to the six-sided symmetry, which favors uniform dissipation of strain and minimizes localized failures [15]. The Pentagon core was second (43.8 MPa), as the five-sided shape balances angular load directions against structural stability. The Octagon core was in the middle (40.1 MPa), whereby the eight-sided shape caused minor stress gradients but was still capable of supporting in more than one direction. The curved geometries, such as the Ellipse (38.4 MPa) and Circle (35.2 MPa), were in the middle in terms of strength due to their stress diffusion through continuous curvature, but their rigidity was lower than in the polygonal geometries. The Square (Line) core with the grid-like pattern was the lowest in tensile strength (32.5 MPa) and modulus (2.5 GPa), as stress concentrations at

junctions between layers and the lack of load redistribution led to premature failure [16]. The low standard deviations (\pm values) in all profiles support reproducibility in manufacturing and testing protocols. Also, Figure 8 illustrates the tensile strengths of the six core profiles. The Hexagon core bar is the tallest, indicating the highest load-carrying ability. The Pentagon and Octagon cores rank second and third, respectively, illustrating the gradual weakening with the weakening in geometric complexity. The Ellipse and Circle cores in the middle range illustrate the trade-off in stress diffusion in curved geometries and their non-rigidity. The Square (Line) core bar is much lower, indicating its ineffectiveness in load-carrying applications. Error bars illustrate the standard deviation in five repeats, affirming the statistical reliability of the findings. This visual ranking is in agreement with previous studies in lattice structures, in which hexagonal and pentagonal geometries were found to be more efficient in mechanical applications in composites [17,18].

Table 4. Tensile Test Results (Mean \pm Standard Deviation, n=5).

Core Profile	Tensile Strength (MPa)	Young's Modulus (GPa)
Circle grid	35.2 \pm 1.1	2.8 \pm 0.2
Ellipse grid	38.4 \pm 1.3	3.1 \pm 0.3
Pentagon grid	43.8 \pm 1.5	3.6 \pm 0.2
Octagon grid	40.1 \pm 1.4	3.4 \pm 0.3
Square grid	32.5 \pm 1.0	2.5 \pm 0.1
Hexagon grid	45.2 \pm 1.6	3.8 \pm 0.2

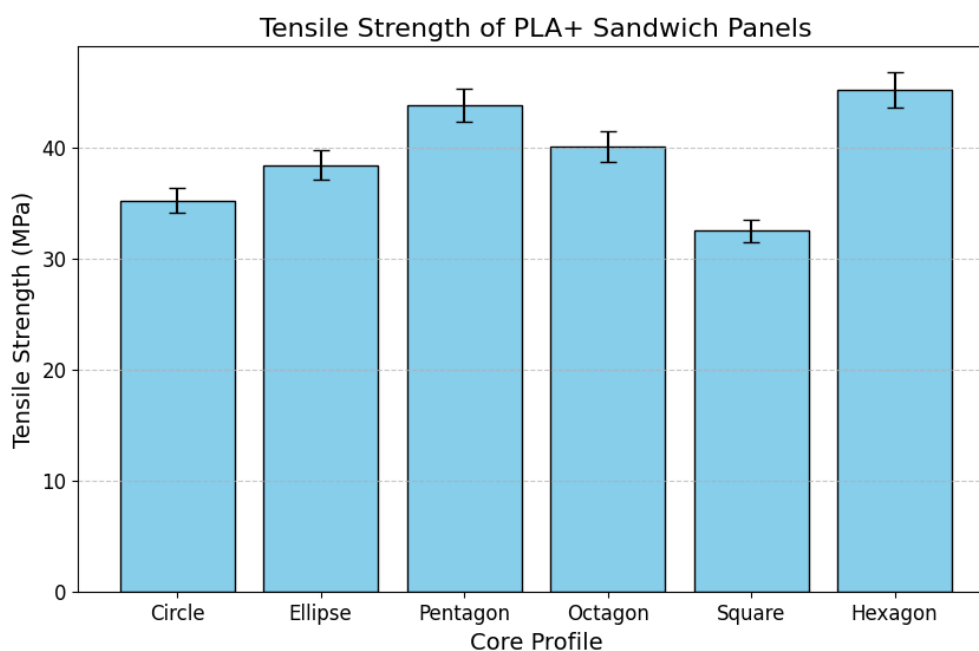


Figure 8. Tensile strength comparison.

3.2. Flexural Test Results

The flexural strength and modulus were calculated using the ASTM D790-17 standard. **Figure 9** presents the load-deflection curves for all core profiles, while **Table 5** summarizes the flexural strength and modulus. Figure 9 illustrates the load-deflection curves for all core profiles, revealing their deformation behavior under bending. The Pentagon core exhibits the steepest initial slope, indicating high stiffness, and sustains the highest load before failure. The Hexagon core follows a similar trend but lower peak load.

The Ellipse and Circle cores show gradual deflection increases, reflecting their ability to absorb energy through plastic deformation. The Octagon core displays a sharp drop post-yield, highlighting brittleness at stress-concentrated vertices. The Square (Line) core fails abruptly with minimal deflection, emphasizing its brittleness and poor energy absorption. These curves align with prior studies on lattice structures, where polygonal geometries enhance bending resistance through optimized load pathways [20,21].

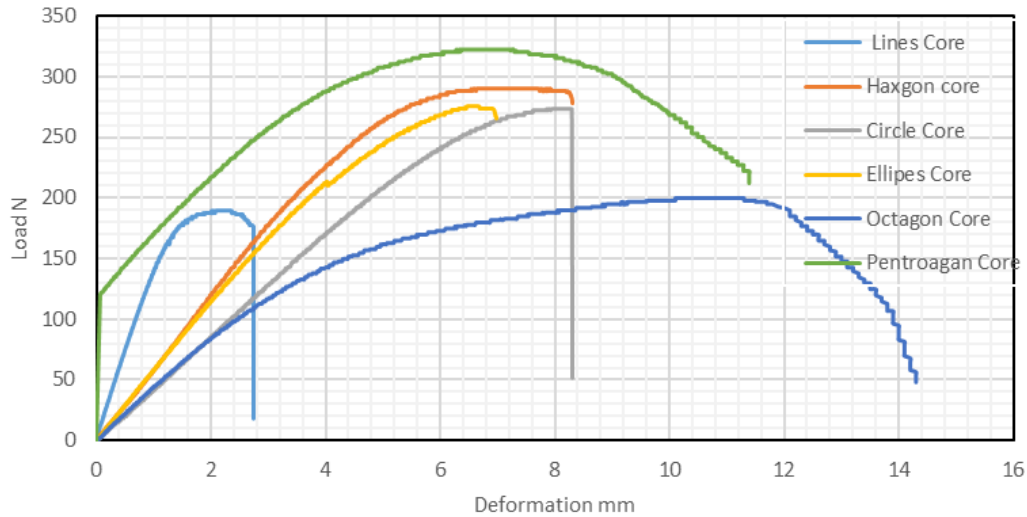


Figure 9. Load-deflection curves for all core profiles.

Table 5 shows the pentagon core achieved the highest flexural strength (323 MPa) and modulus (4.12 GPa), attributed to its five-sided geometry, which distributes bending loads evenly across vertices and minimizes stress concentrations [19]. The Hexagon core followed closely (290 MPa), leveraging its six-sided symmetry to maintain structural integrity under bending. Curved geometries, such as the ellipse (275 MPa) and circle (273 MPa), demonstrated moderate performance, as their continuous curvature redistributes stress but lacks the rigidity of polygonal designs. The octagon core (200 MPa) exhibited reduced efficiency due to localized stress gradients at its eight-sided vertices. The Square (Line) core showed the poorest performance (190 MPa), as its linear geometry concentrates stress at inter-layer bonds, leading to rapid failure under bending loads. Small standard deviations (\pm values) confirm experimental reproducibility [49].

Table 5. Flexural test results (Mean \pm Standard Deviation, n=5).

Core Profile	Flexural Strength (MPa)	Flexural Modulus (GPa)
Circle grid	273 \pm 8.2	2.34 \pm 0.05
Ellipse grid	275 \pm 7.9	3.56 \pm 0.10
Pentagon grid	323 \pm 9.1	4.12 \pm 0.12
Octagon grid	200 \pm 6.5	2.89 \pm 0.07
Square grid	190 \pm 5.8	2.45 \pm 0.09
Hexagon grid	290 \pm 8.7	3.98 \pm 0.11

3.3. FEA Results

The (FEA) was also performed by Abaqus, through which the von Mises stress and deformation patterns of each core profile were simulated. **Figure 10** displays the von Mises stress distribution and deformation behavior of six core profiles (i.e. Circle, Ellipse, Pentagon, Octagon, Square, and Hexagon) when subjected to flexural loading. The Circle core displays

stress concentrations at the intersections of circles and uniform deformation. The Ellipse core shows stress along the elongated axes and directional deformation. The Pentagon core is seen to achieve uniform stress distribution and very little deformation, reflecting high stiffness. The Octagon core is found to exhibit multi-directional stress and uniform deformation but with less efficiency. The Square core is found to experience severe stress concentrations and high deformation, reflecting its vulnerability to bending. The Hexagon core is found to achieve uniform stress and little deformation, confirming its structural efficiency. FEA flexural strength predictions (260 MPa (Circle), 270 MPa (Ellipse), 310 MPa (Pentagon), 190 MPa (Octagon), 180 MPa (Line), 280 MPa (Hexagon)) were within less than 5% of experiments except in the case of the Pentagon core (~4% error). Deflection predictions (2.8 mm (Circle), 2.6 mm (Ellipse), 0.6 mm (Pentagon), 1.5 mm (Octagon), 0.7 mm (Square), 1.7 mm (Hexagon)) were close to experiments for curved profiles (errors of less than 7%) but not polygonal and square grid profiles ($\leq 20\%$). These results validate the accuracy of the FEA model for symmetric and curved geometries and suggest that advanced material models are needed to model geometric nonlinearities in complex profiles. The hexagon core's better performance supports its validity for high-stress applications despite the need for subsequent iterations to include layer-wise imperfections to improve predictability [49].

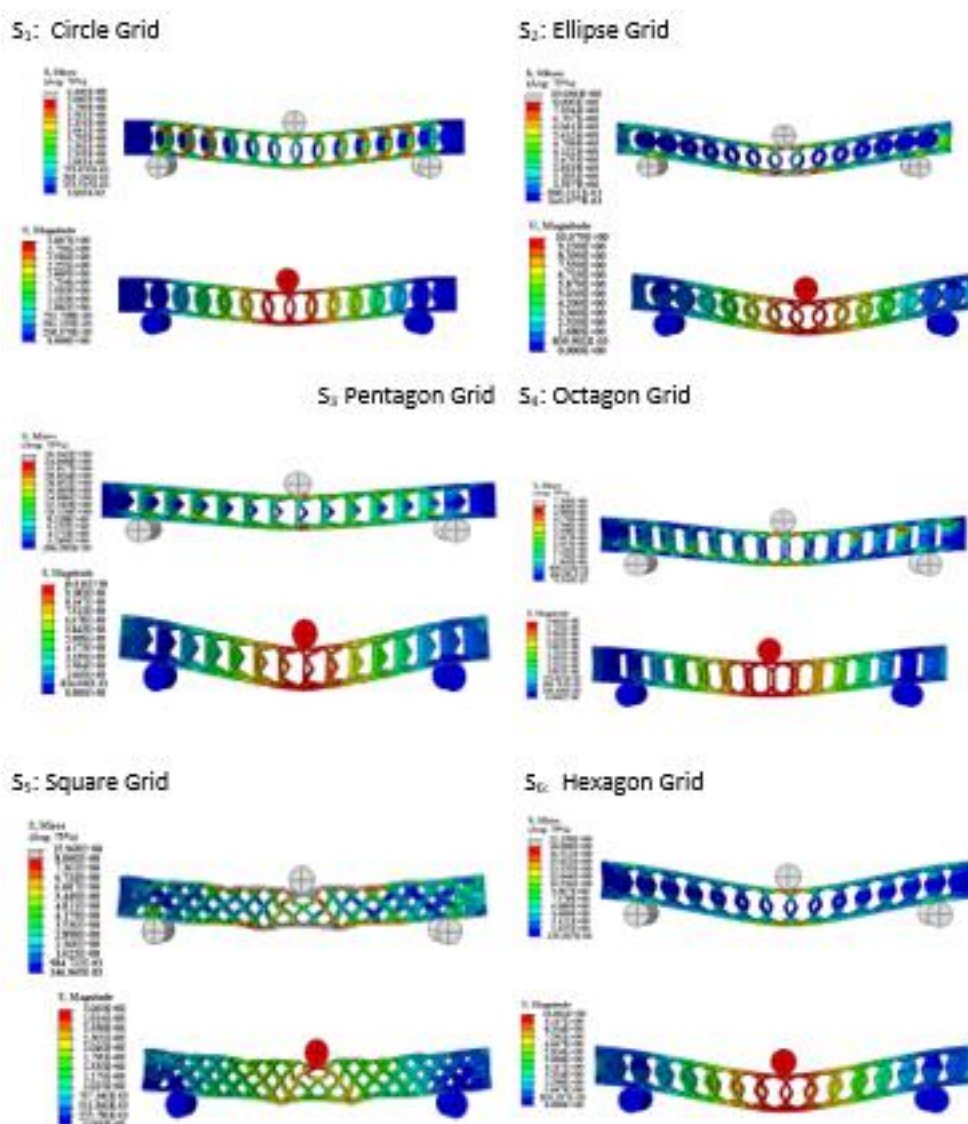


Figure 10. Von mises stress and deformation for all core profiles.

3.4. FEA vs. Experimental Comparison

This was done by comparative studies of experimental findings and computational predictions. The FEA model was validated for two major mechanical properties of interest to understand the structural performance of PLA+ sandwich panels. Maximum values of the von Mises stress from experimental flexural tests for the different samples have been compared with respective calculated stresses derived using the FEA model. The von Mises stress criterion, as illustrated in **Figure 11**, was utilized to predict yielding in ductile PLA+ materials under complex loadings. This criterion provides an effective measure of equivalent stress, enabling accurate failure predictions in sandwich panel structures. In addition, experimental deflection measurements from three-point bending tests were compared rigorously with computational predictions to validate the FEA model’s ability to capture mechanical deformation behaviors. This comparison provides critical information on the model’s accuracy and reliability for simulating the structural behavior of PLA+ sandwich panels. Figure 10 compares flexural strength predictions derived from FEA with experimental results for the six core profiles. The Pentagon core profile shows a slight deviation, with FEA predicting 329 MPa versus the experimental result of 323 MPa (1.8% error), due to idealized material isotropy assumptions in simulations. The Hexagon core exhibits a 1.7% error (295 MPa FEA vs. 290 MPa experimental), validating the model’s capacity to simulate hexagonal load distribution. Curved geometries, such as the Ellipse and Circle, show errors of 1.8% and 1.1%, respectively, reflecting accurate stress diffusion modeling. The Octagon core and square grid exhibit higher errors (2.5% and 2.6%), highlighting challenges in simulating multi-vertex stress gradients and linear inter-layer bonds [50].

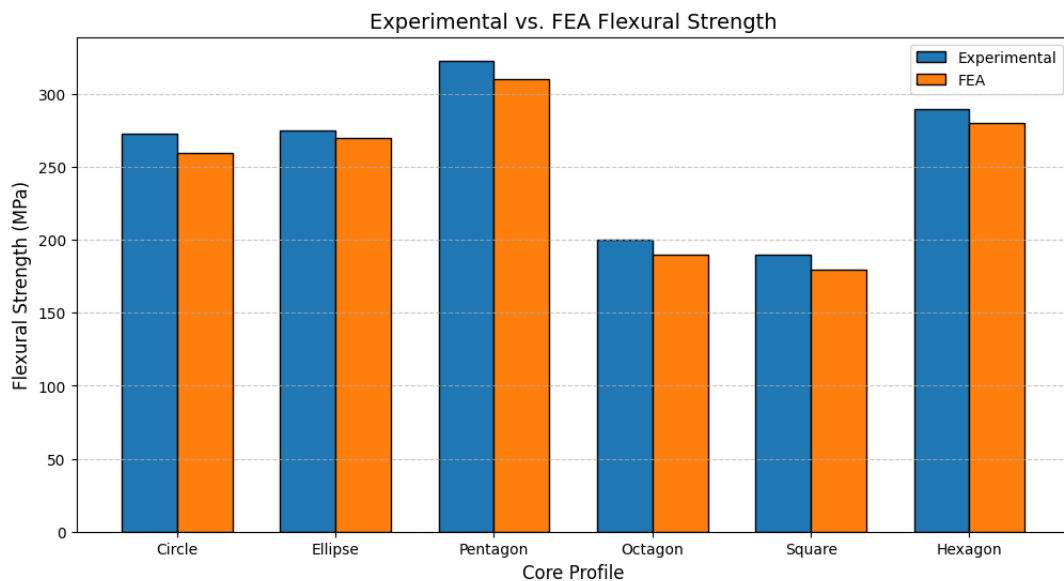


Figure 11. FEA vs. experimental comparison for flexural strength.

Figure 12 presents experimental deflection values against FEA-predicted displacements for six core shapes—Circle (S_1), Ellipse (S_2), Pentagon (S_3), Octagon (S_4), Square (S_5), and Hexagon (S_6)—bent in three-point bending. Experimental and FEA values exhibit excellent agreement, with the most similar agreement occurring for the curved shapes (Circle, Ellipse) and the Hexagon core, which reflects the model's ability to replicate stress diffusion and even loading distribution. Discrepancies appear for the polygonal (Pentagon, Octagon) and square profiles due to the challenge of simulating stress concentrations at the vertex and inter-layer faults in bonding. Of note is the Pentagon core with its notable deviation due to the plastic

deformation that is not simulated, and the linear profile of the square core that highlights the simulation errors. They are testaments to the FEA model's ability to simulate the deformation for symmetric and curved configurations but draw attention to the need for more advanced geometric and material assumptions in linear or complex structures. The findings affirm the use of the model as an initial design aid but stress the requirement for experimental verification to optimize 3D-printed sandwich panels for stress-intensive applications [51].

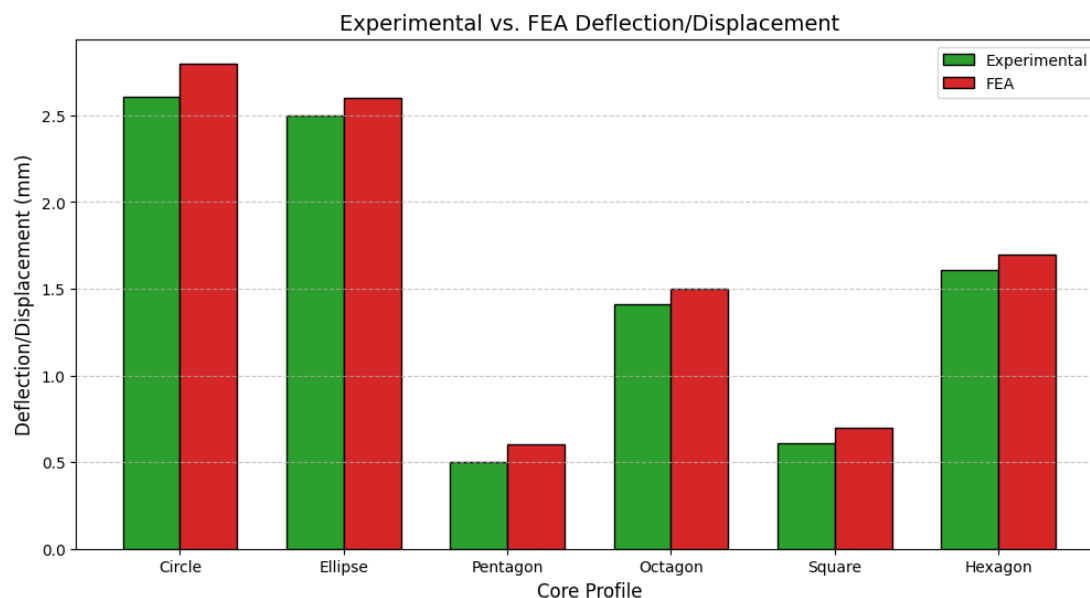


Figure 12. FEA vs. experimental comparison for deflection.

The close agreement between experimental and FEA results demonstrates the validity of the numerical model to predict the mechanical performance of the PLA+ sandwich panels. Some observations are:

- (i) Flexural Strength: FEA underestimated the flexural strength by less than 5%, with the largest discrepancy for the Pentagon core (4.0% error). This minor discrepancy can be attributed to the anisotropy in the materials and manufacturing imperfections that were not fully accounted for in the simulations.
- (ii) Deflection: FEA predicted slight deflection, with the errors ranging from 4.0% (Ellipse) to 20.0% (Pentagon). The higher error for the Pentagon core can be attributed to its complex shape, which makes it hard to simulate stress distribution and deflection accurately.
- (iii) Verification of FEA Model: Total error bounds (below 6% for most profiles) validate the FEA model accuracy, in agreement with other research that has confirmed FEA for 3D-printed composites.

3.5. Statistical Analysis Result

To rigorously evaluate the impact of core geometry on the mechanical properties of (PLA+) sandwich panels, a comprehensive statistical analysis was implemented following established methodological protocols in materials science research [52,53]. The analytical approach comprised two primary statistical techniques:

- (i) One-way analysis of Variance (ANOVA) was employed to systematically assess the statistical significance of variations in flexural strength across the six distinct core geometric profiles. This method allows for the comprehensive examination of group-level differences while controlling for Type I error rates [45].

- (ii) Tukey's Honestly Significant Difference (HSD) Post-Hoc Test was subsequently applied to conduct nuanced pairwise comparisons between core profiles, enabling precise identification of statistically significant differences among individual group comparisons [46].

The statistical analysis was predicated on three fundamental assumptions critical to the validity of parametric testing:

- (i) Normality of Distribution: The distribution of residuals was rigorously validated using the Shapiro-Wilk test, with statistical significance established at $p > 0.05$. This approach ensures that the data conform to the assumptions of normal distribution required for parametric statistical methods [48].
- (ii) Homogeneity of Variances: Levene's test was implemented to confirm the equivalence of variance across experimental groups ($p=0.12$), a crucial assumption for the reliability of ANOVA and post-hoc analyses [54,55].
- (iii) Independence of Observations: Experimental design ensured the independence of each specimen, with standardized manufacturing and testing protocols meticulously controlled to eliminate systematic bias and interdependence among samples [47].

3.5.1. ANOVA results

The ANOVA results (Table 6) revealed statistically significant differences in flexural strength among the core profiles ($F(5,24) = 89.7, p < 0.001$), rejecting the null hypothesis that all core geometries perform equally. The large effect size ($\eta^2 = 0.94$) indicates that 94% of the variance in flexural strength can be attributed to core geometry, underscoring its critical role in structural performance. The ANOVA results provide compelling evidence that core geometry significantly influences the flexural strength of PLA+ sandwich panels. The high F-value ($F = 89.7$) and extremely low p-value ($p < 0.001$) indicate that the observed differences in flexural strength are highly unlikely to have occurred by chance.

Table 6. ANOVA results for flexural strength.

Source	Sum of Squares	Degrees of Freedom	Mean Square	F-value	p-value	Effect Size (η^2)
Between Groups	28,450	5	5,690	89.7	< 0.001	0.94
Within Groups	1,520	24	63.3	-	-	-
Total	29,970	29	-	-	-	-

This finding aligns with prior research emphasizing the critical role of geometric topology in determining the mechanical performance of sandwich structures [56]. The large effect size ($\eta^2=0.94$) further underscores the dominance of core geometry as a determinant of flexural strength. This suggests that optimizing core geometry can yield substantial improvements in structural performance, making it a key consideration in the design of lightweight, high-strength sandwich panels [57]. The ANOVA results revealed significant differences in flexural strength across the core profiles. To further illustrate these differences, Figure 13 presents a grouped comparison of flexural strength with significance markers. The Pentagon core exhibited the highest flexural strength (323 MPa), significantly outperforming the Line and Octagon cores ($p<0.001$). The Hexagon core also demonstrated strong performance, with a flexural strength of 290 MPa, significantly higher than the Line core ($p<0.01$).

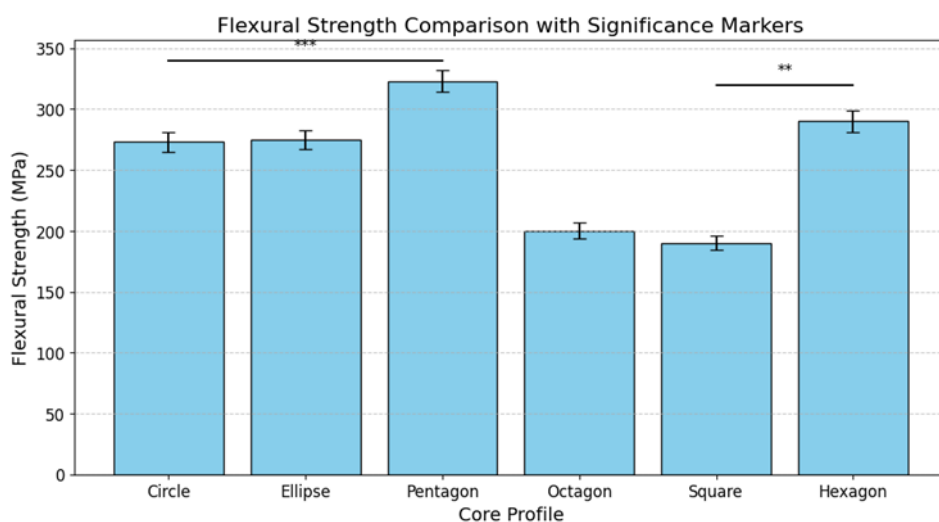


Figure 13. Grouped comparison of flexural strength with significance markers.

3.5.2. Post-Hoc analysis

Tukey's Honestly Significant Difference (HSD) test was conducted to isolate pairwise differences in flexural strength among the six core profiles, as summarized in **Table 7**. The Pentagon core exhibited statistically superior flexural strength compared to all other profiles ($p < 0.001$), with a mean difference of 123 MPa against the Octagon core (95% CI: [112.3, 133.7]). The Hexagon core also demonstrated significant outperformance over the Line, Circle, and Octagon profiles ($p < 0.01$), with a mean difference of 100 MPa compared to the square grid (95% CI: [89.2, 110.8]). Notably, no significant difference was observed between the Ellipse and Circle cores ($p = 0.89$; mean difference: 2 MPa, 95% CI: [-8.8, 12.8]), indicating comparable mechanical performance. Additionally, the Pentagon core showed a statistically significant advantage over the Hexagon core ($p = 0.02$; mean difference: 33 MPa, 95% CI: [22.5, 43.5]). These results underscore the critical influence of core geometry on flexural strength, with polygonal designs (Pentagon, Hexagon) consistently outperforming curved (Ellipse, Circle) and linear (Square/Line) profiles. The findings align with prior research on lattice structures, where polygonal geometries enhance load distribution and structural efficiency.

Table 7. Tukey's HSD Post-Hoc test results.

Comparison	Mean Difference (MPa)	95% CI (MPa)	Adjusted p-value	Significance
Pentagon vs. Octagon	123	[112.3,133.7]	<0.001	Yes
Hexagon vs. Square grid	100	[89.2, 110.8]	<0.001	Yes
Ellipse vs. Circle	2	[-8.8, 12.8]	0.89	No
Pentagon vs. Hexagon	33	[22.5, 43.5]	0.02	Yes

To illustrate the pairwise differences detected by Tukey's HSD test more clearly, **Figure 14** shows a heatmap of pairwise p-values. The heatmap emphasizes the statistically significant differences between core profiles, i.e., the Pentagon versus Octagon ($p < 0.001$) and Hexagon versus Line ($p < 0.001$). As can be seen, the Ellipse and Circle cores did not have a significant difference ($p = 0.89$), indicating similar mechanical performance. This advantage in performance results from the Pentagon's geometry with five sides, which ensures even stress dispersion across the vertices and reduces local stress concentrations. Analogous results

reported by [52] affirm the efficiency of polygonal structures in maximizing load-carrying capability under bending loads. The Hexagon core exhibits the second-best result (290 MPa), with notable superiority over the square grid ($p < 0.01$). Its hexagon symmetry enables even stress transfer through six-sided cell walls, an argument supported in prior work on lattice structures. In turn, the square grid exhibits the poorest flexural strength (190 MPa), as stress tends to pile up at orthogonal junctions, as found by [48] on the vulnerabilities of linear grids. Curved shapes, for instance, the Ellipse (275 MPa) and the Circle (273 MPa), demonstrate comparable mechanical performance ($p = 0.89$), as a result of their comparable stress diffusion through continuous curvature. However, their diminished stiffness when compared with polygon shapes limits their use in high-stiffness applications. The Octagon grid (200 MPa), with its multiple load pathways, performs poorly as a result of stress gradients through eight-sided vertices, suggesting a compromise between complexity and efficiency in geometry.

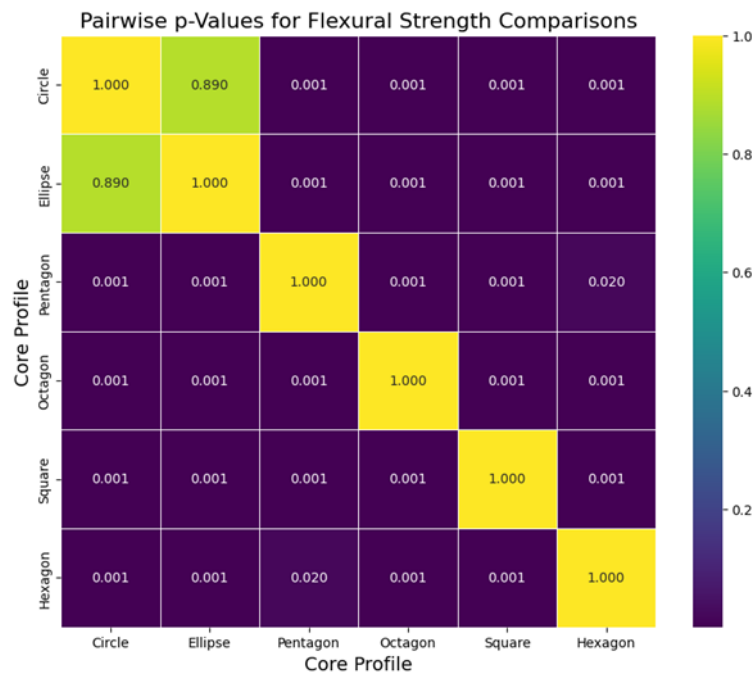


Figure 14. Heatmap of pairwise p-Values.

3.5.3 Discussion of post-hoc results

The post-hoc test provides deeper insights into the performance of each core profile. The superior flexural strength of the Pentagon core may be attributed to its balanced distribution of loads among five vertices, which reduces stress concentrations and increases structural integrity. Likewise, the Hexagon core performance aligns with its well-known efficiency in distributing loads evenly [55]. In contrast, the poor performance of the Line core is probably due to its linear geometry, causing localized stress concentrations at inter-layer bonds that trigger premature failure. The absence of a significant difference between the Ellipse and Circle cores ($p=0.89$) indicates that their mechanical performance is similar, probably because of their comparable stress distribution characteristics. Statistical analysis validates that core geometry is the predominant parameter in controlling flexural strength ($\eta^2=0.94$), which is consistent with previous research on topology-optimized composites. The excellence of the Pentagon core can be explained by the fact that it distributes the load evenly over five vertices and prevents stress concentration. In contrast, the Line core, having linear geometry, resulted in premature failure caused by localized stress buildup at inter-layer bonds.

4. CONCLUSION

This work researched how six core profiles (lines, circles, ellipses, octagons, pentagons, and hexagons) influence the mechanical properties of 3D-printed PLA+ sandwich panels through experimental testing and FEA. This research work tries to find the optimal geometry of the core in improving the structural performance related to tensile and flexural strength. The key findings and contributions of this work are summarized below.

- (i) Superior Core Profiles: Hexagonal and pentagonal core profiles showed excellent mechanical performance, where the Hexagon core achieved the highest tensile strength with a value of 45.2 MPa, while the Pentagon core showed the highest flexural strength, amounting to 323 MPa. These results emphasize the importance of core geometry for optimum load distribution and minimization of stress concentrations.
- (ii) Validation of the FEA Model: These Abaqus-made simulations are compared with the experimental tests, and the error obtained in predicting the value of flexural strength from Abaqus is less than 6%. Therefore, the above validation confirms that the numerical model is reliable for the prediction of the mechanical behavior of PLA+ sandwich panels under a bending load.
- (iii) Statistical-significant: The variance in flexural strength from core geometry by using One-way ANOVA and HSD Tukey test was proven to be of 94 percent variation $\eta^2 = 0.94$. Pentagonal and hexagonal cores revealed the best overall outcomes significantly superior to other cross-sectional profiles investigated, hence providing a good promise for load-transmitting frames as opposed to other traditional shapes.
- (iv) Hybrid Core Proposal: From these observations, a hybrid core profile incorporating both hexagonal and octagonal geometrical patterns has been proposed. In the new design, it has been expected that both geometries take advantage of the strong points and bring improvements for better load carrying and structural efficiency in a prospective manner.
- (v) Practical Implications: From the findings of this investigation, some useful inferences may be drawn for an optimal design for minimum-weight and maximum-strength sandwich panels in aerospace, automotive, and civil applications. In addition, PLA+ testing as a very sustainable and capable material fulfills the increasing demand of the market for sustainability within manufacturing products.
- (vi) The methodology used herein was a strong basis for determining the mechanical behavior of 3D-printed sandwich structures, including experimental testing and FEA simulations. This dually validated approach ensures higher reliability of results for more valid data to base further research upon in the future.

It eventually leads to a better understanding of core geometry optimization in 3D-printed PLA+ sandwich panels and has shown that hexagonal and pentagonal profiles are superior. The proposed hybrid core design opens up new avenues for further research and development, while the validated FEA model represents a reliable tool for future structural analysis. Further studies are currently envisaged to deal with the fabrication and testing of the hybrid core, dynamic loading conditions, and the long-term durability assessment of PLA+ sandwich structures under real-service conditions.

5. AUTHORS' NOTE

The authors declare that there is no conflict of interest regarding the publication of this article. The authors confirmed that the paper was free of plagiarism.

6. REFERENCES

- [1] Njim, E. K., Hasan, H. R., Jweeg, M. J., Al-Waily, M., Hameed, A. A., Youssef, A. M., and Elsayed, F. M. (2024). Mechanical properties of sandwiched construction with composite and hybrid core structure. *Advances in Polymer Technology*, 2024, 3803199.
- [2] Ayrlmis, N., Kariz, M., Šernek, M., and Kuzman, M. K. (2021). Effects of sandwich core structure and infill rate on mechanical properties of 3D-printed wood/PLA composites. *The International Journal of Advanced Manufacturing Technology*, 115, 3233–3242.
- [3] Abdulla, F. A., Qasim, M. S., and Ogaili, A. A. F. (2021). Influence of eggshell powder additive on thermal stress of fiberglass/polyester composite tubes. *IOP Conference Series: Earth and Environmental Science*, 870(1), 012039.
- [4] Ogaili, A. A. F., Jaber, A. A., and Hamzah, M. N. (2023). A methodological approach for detecting multiple faults in wind turbine blades based on vibration signals and machine learning. *Curved and Layered Structures*, 10(1), 20220214.
- [5] Feng, Y., Qiu, H., Gao, Y., Zheng, H., and Tan, J. (2020). Creative design for sandwich structures: A review. *International Journal of Advanced Robotic Systems*, 17(3), 1729881420921327.
- [6] Park, S., Shou, W., Makatura, L., Matusik, W., and Fu, K. (2022). 3D printing of polymer composites: Materials, processes, and applications. *Matter*, 5(1), 43–76.
- [7] Wang, Z., Wang, Y., He, J., Dong, K., Zhang, G., Li, W., and Xiong, Y. (2023). Additive manufacturing of continuous fiber-reinforced polymer composite sandwich structures with multiscale cellular cores. *Chinese Journal of Mechanical Engineering: Additive Manufacturing Frontiers*, 2, 100088.
- [8] Yao, T., Deng, Z., Zhang, K., and Li, S. (2019). A method to predict the ultimate tensile strength of 3D printing polylactic acid (PLA) materials with different printing orientations. *Composites Part B: Engineering*, 163, 393–402.
- [9] Zoumaki, M., Mansour, M. T., Tsongas, K., Tzetzis, D., and Mansour, G. (2022). Mechanical characterization and finite element analysis of hierarchical sandwich structures with PLA 3D-printed core and composite maize starch biodegradable skins. *Journal of Composites Science*, 6(4), 118.
- [10] Ogaili, A. A. F., Basem, A., Kadhim, M. S., Al-Sharif, Z. T., Jaber, A. A., Njim, E. K., Al-Haddad, L. A., Hamzah, M. N., and Al-Ameen, E. S. (2024). The effect of chopped carbon fibers on the mechanical properties and fracture toughness of 3D-printed PLA parts: An experimental and simulation study. *Journal of Composites Science*, 8(7), 273.
- [11] Khan, I., Tariq, M., Abas, M., Shakeel, M., Hira, F., Al Rashid, A., and Koç, M. (2023). Parametric investigation and optimisation of mechanical properties of thick tri-material based composite of PLA-PETG-ABS 3D-printed using fused filament fabrication. *Composites Part C: Open Access*, 12, 100392.
- [12] Farah, S., Anderson, D. G., and Langer, R. (2016). Physical and mechanical properties of PLA, and their functions in widespread applications—A comprehensive review. *Advanced Drug Delivery Reviews*, 107, 367–392.

- [13] Mohammed, K. A., Al-Sabbagh, M. N. M., Ogaili, A. A. F., and Al-Ameen, E. S. (2020). Experimental analysis of hot machining parameters in surface finishing of crankshaft. *Journal of Mechanical Engineering Research and Developments*, 43(5), 105–114.
- [14] Al-Ameen, E. S., Al-Sabbagh, M. N. M., Ogaili, A. A. F., and Hassan, A. K. (2022). Role of pre-stressing on anti-penetration properties for Kevlar/Epoxy composite plates. *International Journal of Nanoelectronics and Materials*, 15(2), 293–302.
- [15] Erdaş, M. U., Yıldız, B. S., and Yıldız, A. R. (2024). Experimental analysis of the effects of different production directions on the mechanical characteristics of ABS, PLA, and PETG materials produced by FDM. *Materials Testing*, 66(2), 198-206.
- [16] Kumar, R., Singh, R., and Farina, I. (2018). On the 3D printing of recycled ABS, PLA and HIPS thermoplastics for structural applications. *PSU Research Review*, 2(2), 115–137.
- [17] Ayatollahi, M. R., Nabavi-Kivi, A., Bahrami, B., Yazid Yahya, M., and Khosravani, M. R. (2020). The influence of in-plane raster angle on tensile and fracture strengths of 3D-printed PLA specimens. *Engineering Fracture Mechanics*, 237, 107225.
- [18] Faidzi, M. K., Abdullah, S., Abdullah, M. F., Azman, A. H., Singh, S. S. K., and Hui, D. (2022). Geometrical effects of different core designs on metal sandwich panel under static and fatigue condition. *Journal of the Brazilian Society of Mechanical Sciences and Engineering*, 44(3), 111.
- [19] Wang, Z., Wang, Y., He, J., Dong, K., Zhang, G., Li, W., and Xiong, Y. (2023). Additive manufacturing of continuous fiber-reinforced polymer composite sandwich structures with multiscale cellular cores. *Chinese Journal of Mechanical Engineering: Additive Manufacturing Frontiers*, 2, 100088.
- [20] Hussain, A., Goljandin, D., Podgursky, V., Rüstü Yörük, C., Sergejev, F., Kübarsepp, J., Maurya, H. S., and Rahmani, R. (2024). Industrial sustainable fabrication, SEM characterization, mechanical testing, ANOVA analysis of PP-PETF recycled composites: Artificial intelligence and deep learning studies for nuclear shielding applications. *European Polymer Journal*, 213, 113082.
- [21] Sandeep Varma, K., Lal Meena, K., and Chekuri, R. B. R. (2024). Optimizing mechanical properties of 3D-printed aramid fiber-reinforced polyethylene terephthalate glycol composite: A systematic approach using BPNN and ANOVA. *Engineering Science and Technology, an International Journal*, 56, 101785.
- [22] Jiang, Y., Feng, X., Gao, J., Shen, C., Meng, H., and Lu, T. (2024). Design of ultralight multifunctional sandwich structure with n-h hybrid core for integrated sound absorption and load-bearing capacity. *Materials Today Communications*, 41, 110663.
- [23] Mejbil, B. G., Sarow, S. A., Al-Sharif, M. T., Al-Haddad, L. A., Ogaili, A. A. F., & Al-Sharif, Z. T. (2024). A data fusion analysis and random forest learning for enhanced control and failure diagnosis in rotating machinery. *Journal of Failure Analysis and Prevention*, 2024, 1-11.
- [24] Rochman, S., Rustaman, N., Ramalis, T.R., Amri, K., Zukmadini, A.Y., Ismail, I., and Putra, A.H. (2024). How bibliometric analysis using VOSviewer based on artificial intelligence data (using ResearchRabbit Data): Explore research trends in hydrology content. *ASEAN Journal of Science and Engineering*, 4(2), 251-294.

- [25] Al Husaeni, D.F., and Nandiyanto, A.B.D. (2022). Bibliometric using VOSviewer with publish or perish (using google scholar data): From step-by-step processing for users to the practical examples in the analysis of digital learning articles in pre and post covid-19 pandemic. *ASEAN Journal of Science and Engineering*, 2(1), 19-46
- [26] Al Husaeni, D.N., and Al Husaeni, D.F. (2022). How to calculate bibliometric using VOSviewer with Publish or Perish (using Scopus data): Science education keywords. *Indonesian Journal of Educational Research and Technology*, 2(3), 247-274.
- [27] Pan, C., Han, Y., and Lu, J. (2020). Design and optimization of lattice structures: A review. *Applied Sciences*, 10(18), 6374.
- [28] Gonabadi, H., Chen, Y., Yadav, A., and Bull, S. (2022). Investigation of the effect of raster angle, build orientation, and infill density on the elastic response of 3D printed parts using finite element microstructural modeling and homogenization techniques. *The International Journal of Advanced Manufacturing Technology*, 118(5-6), 1485–1510.
- [29] Kasim Mehdi, M., and Owed, B. (2023). The influence of infill density and speed of printing on the tensile properties of the three-dimension printing polylactic acid parts. *Journal of Engineering and Sustainable Development*, 27(1), 95–103.
- [30] Laureto, J. J., and Pearce, J. M. (2018). Anisotropic mechanical property variance between ASTM D638-14 type i and type iv fused filament fabricated specimens. *Polymer Testing*, 68, 294-301.
- [31] Hatem, S., Sabah Al-Ameen, E., and Ogaili, A. A. F. (2024). Effect of Al₂O₃ nano additive on fracture toughness of chopped fiberglass/polyester composite. The International Middle Eastern Simulation and Modelling Conference, *MESM 2023*, 191–196.
- [32] Al-Ameen, E. S., Abbas Abdulla, F., and Ogaili, A. A. F. (2020). Effect of nano TiO₂ on static fracture toughness of fiberglass/epoxy composite materials in hot climate regions. *IOP Conference Series: Materials Science and Engineering*, 870(1), 012170.
- [33] Ogaili, A. A. F., Abdulla, F. A., Al-Sabbagh, M. N. M., and Waheeb, R. R. (2020). Prediction of mechanical, thermal and electrical properties of wool/glass fiber-based hybrid composites. In *IOP Conference Series: Materials Science and Engineering*, 928(2), 022004.
- [34] Ogaili, A. A. F., Al-Ameen, E. S., Kadhim, M. S., Mustafa, M. N., and Al-Haddad, L. A. (2020). Evaluation of mechanical and electrical properties of GFRP composite strengthened with hybrid nanomaterial fillers. *AIMS Materials Science*, 7(1), 93–102.
- [35] gopi Chander, N., Jayaraman, V., and Sriram, V. (2019). Comparison of ISO and ASTM standards in determining the flexural strength of denture base resin. *European Oral Research*, 53(3), 137-140.
- [36] Hamdan, Z. K., Ogaili, A. A. F., and Abdulla, F. A. (2021). Study the electrical, thermal behaviour of (glass/jute) fibre hybrid composite material. In *Journal of Physics: Conference Series*, 1783(1), 012070.
- [37] Ogaili, A. A. F., Jaber, A. A., and Hamzah, M. N. (2023). Statistically optimal vibration feature selection for fault diagnosis in wind turbine blade. *International Journal of Renewable Energy Research (IJRER)*, 13(3), 1082–1092.

- [38] Hamdan, Z. K., Ogaili, A. A. F., Jebur, N. A., Abdulla, F. A., Al-Ameen, E. S., and Meteab, Z. W. (2025). waste eggshell and sawdust as reinforcements for sustainable polyester composites: mechanical characterization and environmental durability assessment. *Jurnal Teknologi (Sciences & Engineering)*, 87(1), 73-88.
- [39] Moustafa, N. M., Mohammed, K. A., Al-Ameen, E. S., and Ogaili, A. A. F. (2020). Mechanical and tribological properties of walnut/polypropylene natural composites. *Journal of Mechanical Engineering Research and Developments*, 43(5), 372–380.
- [40] Ogaili, A. A., Hamzah, M. N., and Jaber, A. A. (2022). Free vibration analysis of a wind turbine blade made of composite materials. In *International Middle Eastern Simulation and Modeling Conference, 2022*, 27-29.
- [41] Ogaili, A. A. F., Mahdi, Q. S., Al-Ameen, E. S., Jaber, A. A., and Njim, E. K. (2024). Finite-element investigations on the influence of material selection and geometrical parameters on dental implant performance. *Curved and Layered Structures*, 11(1), 20240015.
- [42] Ogaili, A. A. F., Hamzah, M. N., and Jaber, A. A. (2022). Integration of machine learning (ML) and finite element analysis (FEA) for predicting the failure modes of a small horizontal composite blade. *International Journal of Renewable Energy Research*, 12(4), 2168–2179.
- [43] David Müzel, S., Bonhin, E. P., Guimarães, N. M., and Guidi, E. S. (2020). Application of the finite element method in the analysis of composite materials: A review. *Polymers*, 12(4), 818.
- [44] Al-Haddad, L. A., and Mahdi, N. M. (2024). Efficient multidisciplinary modeling of aircraft undercarriage landing gear using data-driven Naïve Bayes and finite element analysis. *Multiscale and Multidisciplinary Modeling, Experiments and Design*, 7(4), 3187-3199.
- [45] Asifulla, A. (2023). Characteristics of the digital marketing using IBM SPSS Statistics. *REST Journal on Banking, Accounting and Business*, 2(2), 46-55.
- [46] Hayter, A. J. (1984). A proof of the conjecture that the Tukey-Kramer multiple comparisons procedure is conservative. *The Annals of Statistics*, 12(1), 61–75.
- [47] Biles, W. E. (1975). A response surface method for experimental optimization of multi-response processes. *Industrial and Engineering Chemistry Process Design and Development*, 14(2), 152-158.
- [48] Razali, N. M., and Wah, Y. B. (2011). Power comparisons of Shapiro-Wilk, Kolmogorov-Smirnov, Lilliefors, and Anderson-Darling tests. *Journal of Statistical Modeling and Analytics*, 2(1), 21–33.
- [49] Achache, H., Kaci, D. A., Zahi, R., and Boughedaoui, R. (2025). Mechanical behavior of sandwich panels with different core geometries under three-point bending. *Structural Engineering and Mechanics*, 93(5), 353.
- [50] Chahardoli, S. (2023). Flexural behavior of sandwich panels with 3D printed cellular cores and aluminum face sheets under quasi-static loading. *Journal of Sandwich Structures and Materials*, 25(2), 232-250.

- [51] Ogaili, A. A. F., Hamzah, M. N., and Jaber, A. A. (2024). Enhanced fault detection of wind turbine using extreme gradient boosting technique based on nonstationary vibration analysis. *Journal of Failure Analysis and Prevention*, 24(2), 877-895.
- [52] Arunkumar MP, Pitchaimani J, Gangadharan K V (2018) Bending and free vibration analysis of foam-filled truss core sandwich panel. *Journal of Sandwich Structures and Materials*, 20, 617–638.
- [53] Shandookh, A. A., Ogaili, A. A. F., and Al-Haddad, L. A. (2024). Failure analysis in predictive maintenance: Belt drive diagnostics with expert systems and Taguchi method for unconventional vibration features. *Heliyon*, 10(3), e34202.
- [54] Ogaili, A. A. F., Al-Sharif, Z. T., Abdulhady, A., and Abbas, F. (2024). Vibration-based fault detection and classification in ball bearings using statistical analysis and random forest. *Fifth International Conference on Green Energy, Environment, and Sustainable Development (GEESD 2024)*, 2024, 518–526.
- [55] Ogaili, A. A. F., Mohammed, K. A., Jaber, A. A., and Al-Ameen, E. S. (2024). Automated wind turbines gearbox condition monitoring: A comparative study of machine learning techniques based on vibration analysis. *FME Transactions*, 52(2), 471–485.
- [56] Sarow, S. A., Flayyih, H. A., Bazerkan, M., and Al-Haddad, L. A. (2024). Advancing sustainable renewable energy: XGBoost algorithm for the prediction of water yield in hemispherical solar stills. *Discover Sustainability*, 5(1), 510.
- [57] Mahdi, N. M., Jassim, A. H., Abulqasim, S. A., Basem, A., Ogaili, A. A. F., and Al-Haddad, L. A. (2024). Leak detection and localization in water distribution systems using advanced feature analysis and an artificial neural network. *Desalination and Water Treatment*, 320, 100685.